Dynamic Analysis of Iris Configuration with Anterior Segment Optical Coherence Tomography

Carol Yim-lui Cheung,[1] *Shu Liu,*[1] *Robert N. Weinreb,*[2] *Jing Liu,*[1] *Haitao Li,*[1] *Dexter Yu-lung Leung,*[1] *Syril Dorairaj,*[2,3] *Jeffrey Liebmann,*[3,4] *Robert Ritch,*[3,5] *Dennis Shun Chiu Lam,*[1] *and Christopher Kai-shun Leung*[1]

Purpose. To evaluate dynamic changes in iris configuration and their association with anterior chamber angle width by using anterior segment optical coherence tomography (ASOCT).

Methods. Forty-six normal subjects with open angles and 40 with narrow angles (Shaffer grade ≤2 in three or more quadrants during dark room gonioscopy) were analyzed. The dynamic ASOCT dark–light changes of iris bowing were captured with real-time video recording and nasal iris bowing, nasal anterior chamber angle, and pupil diameter were measured in serial image frames selected from the video capture. The associations between iris bowing, iris thickness, anterior chamber depth (ACD), age, anterior chamber angle, and pupillary diameter measurements were evaluated with univariate and multivariate regression analyses.

Results. The relationship between iris bowing and pupil diameter was largely linear, with three dynamic patterns observed: (1) convex-to-convex (iris remains convex in dark and light); (2) concave-to-convex (iris changes from concave to convex from light to dark); and (3) concave-to-concave (iris remains concave in dark and light). All the subjects with narrow angles had convex-to-convex anatomy, although 43% of the subjects with open angles also demonstrated this pattern. These individuals were older and had shorter axial length (both with $P < 0.001$). Older age ($r = -0.352$, $P = 0.001$), smaller ACD ($r = 0.382$, $P < 0.001$), and smaller difference in angle opening distance in light and dark ($r = 0.472$, $P < 0.001$) were associated with smaller differences in iris bowing in the light and dark. ACD and iris bowing were independently associated with anterior chamber angle width.

Conclusions. Independent of ACD, iris bowing is an important biometric parameter that determines angle width. Investigation of iris dynamics may offer a new perspective in understanding the risk and mechanism of primary angle closure.

From the [1]Department of Ophthalmology and Visual Sciences, The Chinese University of Hong Kong, Hong Kong, Peoples Republic of China; the [2]Hamilton Glaucoma Center, University of California, San Diego, California; the [3]Einhorn Clinical Research Center, New York Eye and Ear Infirmary, New York, New York; the [4]NYU School of Medicine, New York, New York; and the [5]Department of Ophthalmology, The New York Medical College, Valhalla, New York.

Submitted for publication May 1, 2009; revised October 29, 2009; accepted January 12, 2010.

Disclosure: **C.Y. Cheung**, None; **S. Liu**, None; **R.N. Weinreb**, Carl Zeiss Meditec (F, C); **J. Liu**, None; **H. Li**, None; **D. Y. Leung**, None; **S. Dorairaj**, None; **J. Liebmann**, None; **R. Ritch**, None; **D.S.C. Lam**, None; **C.K. Leung**, Carl Zeiss Meditec (F, R)

Corresponding author: Christopher Kai-shun Leung, Department of Ophthalmology and Visual Sciences, The Chinese University of Hong Kong, Hong Kong, Peoples Republic of China; tlims00@hotmail.com.

(*Invest Ophthalmol Vis Sci.* 2010;51:4040–4046) DOI: 10.1167/iovs.09-3941

Primary angle-closure glaucoma is a major cause of visual morbidity in East Asia.[1,2] Several biometric risk factors, including shallow anterior chamber depth (ACD), short axial length, and small corneal diameter have been related to the development of primary angle closure (PAC),[3–8] but less attention has been focused on the iris, because it is difficult to quantify its dimensions with either slit lamp biomicroscopy or gonioscopy. The iris is a dynamic structure, constantly changing in configuration in response to light and accommodation. Standardizing of lighting conditions and accommodation is crucial for objective measurement of iris dimensions.

Analysis of iris bowing has been investigated with ultrasound biomicroscopy (UBM).[9–11] UBM, however, is limited because it is a contact technique. Anterior segment optical coherence tomography (ASOCT) is a noncontact imaging method that provides cross-sectional visualization of the anterior segment. With a scan speed of 2000 A-scans per second and the ability to adjust the focus of the internal fixation target, dynamic changes in iris bowing can be imaged and objectively measured in dark and light without being influenced by accommodation. In this study, we evaluated dynamic changes of iris configuration and their association with the anterior chamber angle (ACA).

Methods

The study was conducted in accordance with the ethics stated in the 1964 Declaration of Helsinki and approved by the local Clinical Research Ethics Committee. After the purpose and nature of the investigation were explained, informed consent was obtained from 86 Chinese subjects (46 with open angles and 40 with narrow angles), who were under observation in the Department of Ophthalmology, Hong Kong Eye Hospital. All subjects underwent a complete ophthalmic examination including visual acuity with refraction, A-scan UBM, slit lamp biomicroscopy, intraocular pressure measurement, and fundus examination. Except for cataract, these subjects had no evidence of ocular disease or glaucoma. Indentation gonioscopy was performed with a short and narrow beam width of the minimum possible illumination in a completely darkened room with a four-mirror indentation gonioprism. Caution was used to avoid having the slit beam light fall on the pupil. A modified Shaffer grading system was used to describe the angle width.[12] A narrow angle was defined as Shaffer grade ≤2 in three or more quadrants during dark room gonioscopy. Subjects with evidence of peripheral anterior synechiae on indentation, a history of the use of any topical or systemic medication that could affect the ACA or pupillary reflex, or a history of previous intraocular operative or laser surgery, were excluded from the study.

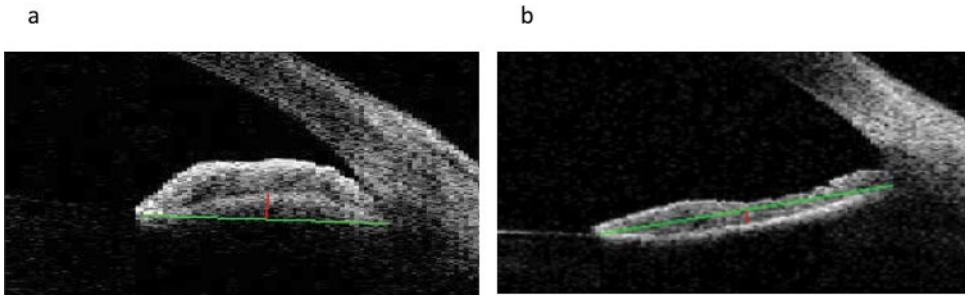

FIGURE 1. Measurement of iris bowing in eyes with convex (**a**) and concave (**b**) irises. Iris bowing (*red line*) was defined as the perpendicular distance from the iris pigment epithelium to a midpoint between the iris root and the iris tip (the contact point between the iris and the lens at the pupillary margin; *green line*).

ASOCT Imaging

In a randomly selected eye, ASOCT imaging was performed with a Visante OCT (model 1000; Carl Zeiss Meditec, Inc., Dublin, CA). The system's principle of imaging is based on low-coherence interferometry, with a 1310-nm superluminescent light-emitting diode (SLD) as the light source. Analogous to an ultrasound B-scan, the Visante OCT acquires multiple A-scans and aligns them to construct two-dimensional images. The scanning of the anterior segment was a noncontact procedure during which the subject fixated on an internal target with focus adjusted with reference to the subject's refractive error at distance. The Visante OCT allows real-time imaging of the anterior chamber with a scan speed of 2000 A-scans per second. The scan acquisition time is 0.125 second per line for the anterior segment single scan (limbal-to-limbal) at eight frames per second. The detail of video recording with ASOCT imaging has been described.[13] In brief, an OCT scan line (anterior segment single 0° to 180°, 6 mm deep × 16 mm wide, and 256 A-scans per line) was manually adjusted to bisect the pupil, with video recording began once the subject had been dark adapted for approximately 1 minute. The video capture was performed in the dark (light intensity measured at the subject's sitting location, 0.3 lux) and the room light was then turned on (light intensity, 368 lux). The change in pupil diameter, from dilation in dark to constriction under room light, and the associated changes in iris configuration were recorded in a video file that was subsequently exported for editing. Each video file was reviewed in video editing software (Video Edit Magic ver. 4.21; Deskshare, Melville, NY). The image series in each eye was then reviewed frame by frame, and the images that showed changes in pupil diameter compared with the preceding images were selected for iris and angle measurements. The average number of image frames analyzed per eye was 9.2 (range, 5–16). Seven subjects were excluded because of difficulty in identifying the scleral spur in one or more image frames in the video capture, and two were excluded because of suboptimal video quality related to eye blinking and eye movement. Only the nasal iris and nasal angle were measured.

Measurement of ACA Width and Pupil Diameter

A program was written in commercial software (MatLab ver. 6.5; The MathWorks, Natick, MA) for the measurement of the angle-opening distance (AOD), the trabecular–iris angle (TIA), and the trabecular–iris space area (TISA) after manual selection of the locations of the scleral spur and apex of the iris recess. Good reliability of angle measurement has been shown with this program (the intra- and interobserver intraclass correlation coefficients [ICC] for ACA measurement ranged between 0.95–0.98 and 0.97–0.99, respectively).[14,15] AOD 500 was calculated as the distance from the corneal endothelium to the anterior iris surface, perpendicular to a line drawn at 500 μm from the scleral spur. The TIA 500 was defined as an angle measured with the apex in the iris recess with the arms of the angle passing through a point on the trabecular meshwork 500 μm from the scleral spur and a point on the iris located perpendicularly. The TISA 500 is an area bounded anteriorly by the AOD 500, posteriorly by a line drawn from the scleral spur perpendicular to the plane of the inner scleral wall to the opposing iris,

TABLE 1. Comparisons of Biometric Parameters in the Open- and Narrow-Angle Groups

	Open Angle, Mean (95% CI) (n = 46)	Narrow Angle, Mean (95% CI) (n = 40)	P*
Age, y	52.41 (46.60 to 58.22)	67.03 (63.99 to 70.06)	<0.001
Spherical equivalent, D	−1.23 (−2.00 to −0.45)	0.77 (0.04 to 1.49)	<0.001
Axial length, mm	24.29 (23.93 to 24.66)	22.95 (22.62 to 23.28)	<0.001
Anterior chamber depth, mm	2.86 (2.74 to 2.98)	2.15 (2.06 to 2.25)	<0.001
Pupil diameter$_{(dark)}$, mm	5.30 (4.93 to 5.67)	4.84 (4.51 to 5.17)	0.068
Pupil diameter$_{(light)}$, mm	3.25 (2.98 to 3.53)	3.05 (2.80 to 3.30)	0.270
AOD$_{(dark)}$, mm	0.434 (0.383 to 0.485)	0.178 (0.123 to 0.233)	<0.001
AOD$_{(light)}$, mm	0.622 (0.561 to 0.682)	0.337 (0.272 to 0.402)	<0.001
TIA$_{(dark)}$, deg	32.0 (29.0 to 35.1)	14.5 (11.2 to 17.8)	<0.001
TIA$_{(light)}$, deg	42.1 (39.3 to 44.8)	25.4 (22.5 to 28.4)	<0.001
TISA$_{(dark)}$, mm^2	0.145 (0.126 to 0.164)	0.060 (0.039 to 0.080)	<0.001
ISA$_{(light)}$, mm^2	0.222 (0.201 to 0.242)	0.118 (0.096 to 0.141)	<0.001
Iris bowing$_{(dark)}$, mm	0.209 (0.181 to 0.237)	0.312 (0.282 to 0.342)	<0.001
Iris bowing$_{(light)}$, mm	0.082 (0.057 to 0.107)	0.196 (0.169 to 0.222)	<0.001
Iris thickness$_{(dark)}$, mm	0.451 (0.431 to 0.471)	0.442 (0.420 to 0.463)	0.541
Iris thickness$_{(light)}$, mm	0.431 (0.409 to 0.453)	0.422 (0.399 to 0.446)	0.617

95% CI, 95% confidence interval.

* Comparisons of anterior chamber angle and iris parameters have been adjusted for age and pupil size.

Table 2. Univariate and Multivariate Regression Analyses between Age, Axial Length, Anterior Chamber Depth, Iris Bowing, Iris Thickness (Independent Variables), and AOD Measured in the Dark (Dependent Variable)

	Unstandardized Coefficients, β (95% CI)	Standardized Coefficients, β	R^2	P
Univariate analysis				
Age, y	−0.008 (−0.011 to −0.006)	−0.580	0.337	<0.001
Axial length, mm	0.117 (0.085 to 0.148)	0.626	0.392	<0.001
Anterior chamber depth, mm	0.392 (0.330 to 0.455)	0.807	0.651	<0.001
Iris bowing$_{(dark)}$, mm	−1.434 (−1.676 to −1.192)	−0.789	0.623	<0.001
Iris thickness$_{(dark)}$, mm	0.161 (−0.650 to 0.973)	0.043	0.002	0.694
Pupil diameter$_{(dark)}$, mm	0.065 (0.022 to 0.109)	0.309	0.095	0.004
Multivariate analysis				
Age, y	−0.001 (−0.003 to 0.001)	−0.065	—	0.435
Anterior chamber depth, mm	0.251 (0.162 to 0.340)	0.517	—	<0.001
Iris bowing$_{(dark)}$, mm	−0.701 (−1.058 to −0.344)	−0.386	—	<0.001
Pupil diameter$_{(dark)}$, mm	−0.019 (−0.047 to 0.010)	−0.090	—	0.193
$R^2 = 0.732$; $P < 0.001$				

superiorly by the inner corneoscleral wall, and inferiorly by the iris surface.[16] Pupil diameter was determined as the distance between the pupil margins. ACD was measured in the ASOCT images as the perpendicular distance from the anterior surface of the lens to the corneal endothelium.

Measurement of Iris Thickness and Iris Bowing

Image analysis software (SigmaScan Pro ver. 5.0; Systat Software, Inc., Point Richmond, CA) was used to measure iris thickness and iris bowing. Iris thickness was the distance between the anterior and posterior iris surfaces at the midpoint between the iris root and the iris tip. Iris bowing was defined as the perpendicular distance from the iris pigment epithelium to a midpoint between the iris root and the iris tip (the contact point between the iris and the lens at the pupillary margin).[10–11] As the point of greatest concavity or convexity may vary from frame to frame in a video capture, the midpoint between the iris root and the iris tip was selected as the reference landmark, to reduce the measurement variability of iris bowing. If the line of measurement was posterior to the iris pigment epithelium (Fig. 1a), the sign of iris bowing was positive, and the iris was anteriorly convex. If the line of measurement was anterior to the iris pigment epithelium (Fig. 1b), the sign of iris bowing was negative, and the iris was anteriorly concave. Thirty images from 30 subjects (15 with convex irises and 15 with concave ones) were randomly selected for evaluation of measurement reliability of iris bowing. The intra- and interobserver ICCs were 0.98.

Statistics

Age, axial length, spherical equivalent, and pupil diameter between the open- and narrow-angle groups were compared by independent *t*-test after checking the assumption of normality (SPSS version 15.0; SPSS, Chicago, IL). ACA and iris parameters (ACD, AOD, TIA, TISA, iris bowing, and iris thickness) were compared with adjustment of age and pupil size. The relationship between iris bowing and pupil diameter in each eye was studied with linear regression analysis. Univariate and multivariate regression analyses were performed to determine factors (age, axial length, ACD, and iris thickness) associated with AOD and iris bowing measured in the dark. Factors significant at $P < 0.05$ were included in the multivariate analysis. The associations between the difference in iris bowing in light and dark (iris bowing$_{(dark)}$ minus iris bowing$_{(light)}$) and the differences in AOD/TIA/TISA (angle width$_{(light)}$ minus angle width$_{(dark)}$) in light and dark, age, axial length, ACD, and iris thickness were examined with univariate regression analysis.

Results

Forty-six subjects with open angles and 40 with narrow angles were included. Table 1 compares the biometric parameters between the open- and narrow-angle groups. The axial length, ACD, and ACA measurements were significantly smaller, and the iris bowing was significantly greater in the narrow-angle group (all with $P < 0.001$). In both open- and narrow-angle subjects, the ACA measurements were greater in the light than in the dark, and iris bowing was more positive, or less negative, in the dark (all with $P < 0.001$). No significant difference was observed in iris thickness between the two groups. Although AOD was significantly associated with age, axial length, ACD, and iris bowing (all with $P < 0.001$), ACD, and iris bowing were the only two factors independently associated with the ACA measurements in the multivariate analyses (both with $P \leq 0.001$; Table 2).

The distribution of subjects with convex or concave iris configurations in dark and in light in the open- and narrow-angle groups is shown in Table 3. Three different dynamic patterns (1) convex-to-convex, (2) concave-to-convex, and (3) concave-to-concave were observed in the relationship between iris bowing and pupil diameter (Fig. 2). Convex-to-convex represents a configuration in which the iris remains convex in changing from the light to the dark (Fig. 2a). For concave-to-convex configuration, the iris changes from concave in the light to convex in the dark (Fig. 2b). For concave-to-concave configuration, the iris remains concave when changing from the light to the dark (Fig. 2c). The relationship between iris bowing and pupil diameter was largely linear; 95.7% ($n = 44$) of open-angle subjects and 92.5% ($n = 37$) of narrow-angle subjects showed significant ($P < 0.05$) linear association between iris bowing and pupil diameter. The direction of association was the same for the three dynamic patterns: An increase in pupil diameter was associated with an increase in iris convexity. All subjects in the narrow-angle group had a convex-to-convex configuration. Of the subjects with open angles, 65.2% had convex-to-convex, 21.7% had concave-to-convex, and 13.0% had concave-to-concave configurations. In eyes with

Table 3. Distribution of Iris Configurations, in Dark and in Light, in the Open- and Narrow-Angle Groups

Iris Configurations	Open Angle ($n = 46$)	Narrow Angle ($n = 40$)
In dark		
Concave	6 (13)	0 (0)
Convex	40 (87)	40 (100)
In light		
Concave	16 (35)	0 (0)
Convex	30 (65)	40 (100)

Data are expressed as *n* (%).

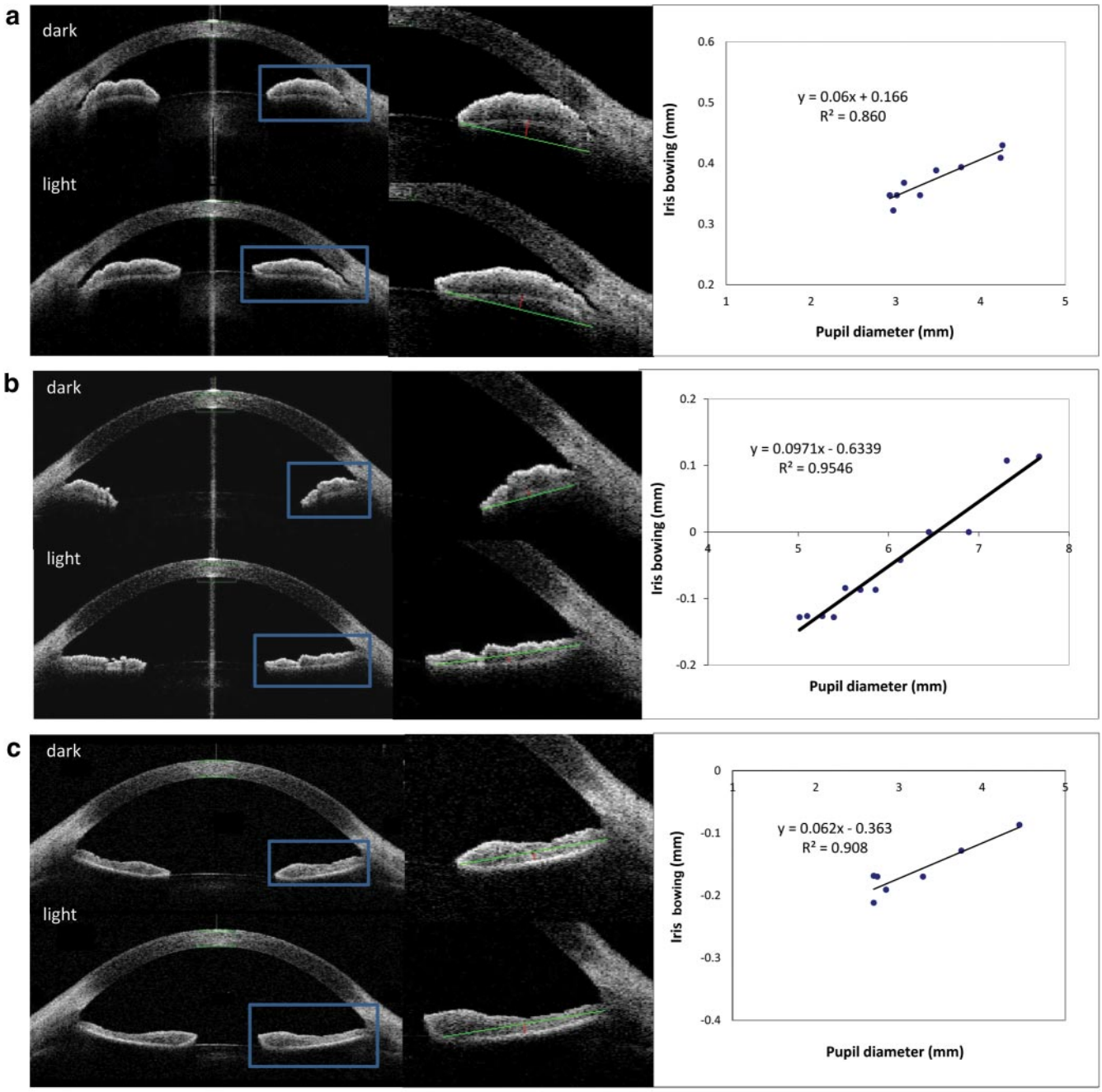

Figure 2. The dynamic patterns of iris bowing in light and dark. (**a**) Convex-to-convex represents a configuration in which the iris remains in convexity from light to dark. (**b**) The iris with concave-to-convex configuration changes from concavity in light to convexity in dark. (**c**) The iris with concave-to-concave configuration remains in concavity from light to dark. *Left*: horizontal ASCOT image captured in dark (*top*) and in light (*bottom*). The nasal sides (outlined in *blue*) were analyzed. *Middle*: an enlarged view showing the measurement of iris bowing (*red line*). *Right*: linear regression analysis between iris bowing and pupil diameter.

Table 4. Comparison of Iris Parameters between the Open- and Narrow-Angle Groups with Convex-to-Convex Iris Configuration

	Open Angle, Mean (95% CI) (n = 30)	Narrow Angle, Mean (95% CI) (n = 40)	P*
Iris bowing$_{(dark)}$, mm	0.255 (0.226 to 0.284)	0.338 (0.313 to 0.363)	<0.001
Iris bowing$_{(light)}$, mm	0.140 (0.113 to 0.166)	0.229 (0.207 to 0.252)	<0.001
Iris thickness$_{(dark)}$, mm	0.449 (0.424 to 0.474)	0.439 (0.417 to 0.461)	0.557
Iris thickness$_{(light)}$, mm	0.436 (0.409 to 0.463)	0.426 (0.403 to 0.449)	0.581

* Comparison adjusted for pupil diameter and age.

convex-to-convex configuration, the iris was more convex in the narrow-angle group than in the open-angle group, although iris thickness was not significantly different between the groups (Table 4). The dynamic patterns of iris bowing were significantly related to age and axial length. Subjects with convex-to-convex configuration were older and had shorter axial length compared with those with concave-to-concave or concave-to-convex configurations (Mann-Whitney test, both with $P < 0.001$; Figs. 3a, 3b). Iris thickness was not significantly different among the groups (Figs. 3c, 3d).

Table 5 shows the association between age, axial length, ACD, ACA measurements, iris thickness, and the difference in iris bowing in light and dark (iris $\text{bowing}_{(\text{dark})}$ minus iris $\text{bowing}_{(\text{light})}$). Older age ($r = -0.352$, $P = 0.001$), smaller ACD ($r = 0.382$, $P < 0.001$), and a smaller difference in angle width were associated with a smaller difference in iris bowing.

Discussion

With real-time ASOCT recording, we observed three different dynamic patterns of iris configuration. These patterns were related to age, axial length, and the ACA. The convex-to-convex configuration was found predominantly in older subjects with shorter axial length. All subjects in the narrow-angle group had convex-to-convex configuration. Individuals with concave-to-concave or concave-to-convex configurations were younger and had longer axial length. The importance in iris bowing in determining the ACA is reflected by the observation that both the iris bowing and ACD were independently associated with the angle width.

The presence of iris convexity has been attributed to the existence of aqueous outflow resistance at the pupillary margin, generating a pressure gradient between the anterior and posterior chambers.[17] In agreement with a recent study using UBM,[11] we found that increased age and decreased ACD were significantly associated with increased iris bowing. In addition, we showed that both iris bowing and ACD were independently associated with the angle width. This finding suggests that in addition to ACD, the iris configuration plays an important role in determining the angle width and the risk of angle closure. With aging, the lens gradually moves forward, pushing the iris diaphragm anteriorly and causes a closer contact between the iris and the lens. It is probable that iris convexity increases as a result of increased relative pupillary block.[11] It has been shown that the anterior bowing of the iris in PAC resumes a flattened configuration after laser iridotomy when the pressure in the anterior and posterior chambers is equalized.[18,19] Iris bowing may serve to signify the degree of relative pupillary block. Both ACD and iris bowing measurements are essential in understanding the risk and mechanism of PAC.

Posterior bowing of the iris (or iris concavity) has been described by UBM imaging in subjects during eye accommodation and in patients with pigment dispersion syndrome.[20,21] Although it is difficult to control for accommodation (particularly in younger individuals) during UBM imaging, the Visante ASOCT minimizes the influence of accommodation by adjusting the focus of the internal fixation target with reference to the subject's refractive error at distance. In this study, iris concavity was found in normal subjects when the eyes were not accommodating. In addition, iris concavity was more frequently observed in the light when the pupil was constricted (10 subjects had the pattern of concave-to-convex configuration). All subjects demonstrating iris concavity (in light and/or in dark) had open angles, were younger, and had longer axial length. None of them had evidence of pigment dispersion syndrome. The mechanism of iris concavity in pigment dispersion syndrome has been attributed to iridozonular contact

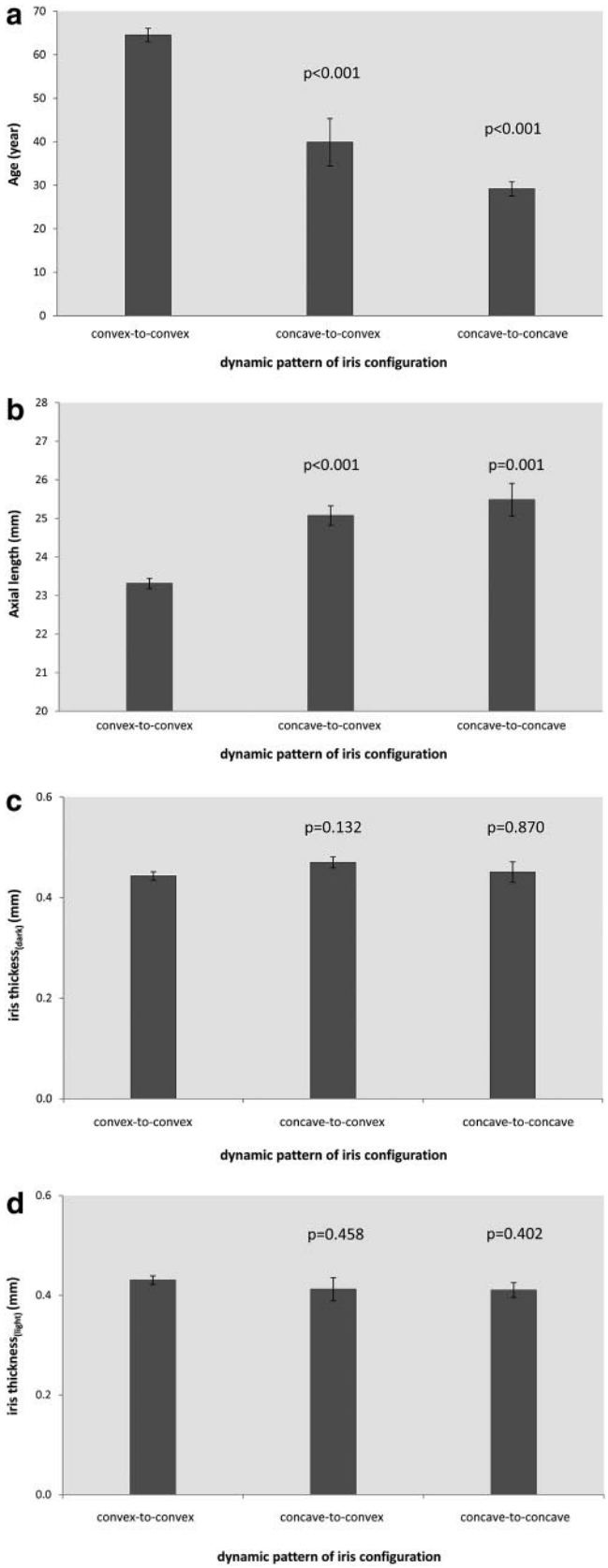

Figure 3. Bar charts demonstrating the relationships between different dynamic patterns of iris configuration and (**a**) age, (**b**) axial length and iris thickness in (**c**) dark and (**d**) light.

TABLE 5. Univariate Analysis between Age, Axial Length, Anterior Chamber Depth, Iris Thickness, the Difference of ACA Measurements in Dark and Light (Independent Variables) and the Difference of Iris Bowing Measurements in Dark and Light (Dependent Variable)

	Unstandardized Coefficients, β (95% CI)	Standardized Coefficients, β	R^2	P
Age, y	−0.0013 (−0.0006 to −0.002)	−0.352	0.124	0.001
Axial length, mm	0.006 (−0.005 to 0.017)	0.114	0.013	0.298
Anterior chamber depth, mm	0.050 (0.024 to 0.076)	0.382	0.146	<0.001
Difference of AOD ($AOD_{(light)} - AOD_{(dark)}$), mm	0.272 (0.162 to 0.382)	0.472	0.223	<0.001
Difference of TIA ($TIA_{(light)} - TIA_{(dark)}$), deg	0.005 (0.002 to 0.007)	0.403	0.162	<0.001
Difference of TISA ($TISA_{(light)} - TISA_{(dark)}$), mm^2	0.843 (0.481 to 1.206)	0.450	0.203	<0.001
Iris $thickness_{(dark)}$, mm	0.071 (−0.147 to 0.289)	0.070	0.005	0.521

resulting in reverse pupillary block.[22] In normal subjects, it has been proposed that forward movement of the lens during accommodation causes temporary reduction of the anterior chamber volume, and the increase in anterior chamber pressure pushes the iris back.[23,24] Although it remains unclear what causes iris concavity in nonaccommodating eyes, the observation that iris concavity was reduced from light to dark suggests that the pressure gradient across the anterior and posterior chambers varies with pupil diameter, resulting in different iris configurations. When the pupil is dilated from light to dark, there is an abrupt reduction in posterior chamber volume, leading to an increase in the posterior chamber pressure (assuming the outflow resistance at the pupillary margin is constant).

This pressure change pushes the iris to adopt a less concave or even a convex configuration. Likewise, in subjects with a convex iris in light, the convexity increases when the pupil is dilated in the dark. Dynamic measurement of iris bowing may offer an effective approach to the study of the change in pressure differential across the iris.

All narrow-angle subjects had convex-to-convex iris configuration. In fact, the increase in iris bowing from light to dark contributed to the increased narrowing of the angle when the pupil was dilated (Table 3). For this reason, it is important to examine the angle in the dark for evaluation of angle closure. It is notable that not all subjects with convex-to-convex configuration had narrow angles (43% had open angles). Although anterior bowing of the iris indicates the presence of relative pupillary block and is a key factor in determining angle width, iris configuration should always be interpreted with reference to other biometric risk factors for angle closure. The difference in iris bowing in light and dark correlated negatively with age and positively with ACD. It is plausible that the iris becomes stiffer in older subjects and in subjects with smaller ACD. This notion is in agreement with a recent study showing that collagen density is increased in eyes with PAC.[25] Age and ACD are known risk factors for PAC. It would be interesting to investigate whether a stiff iris is also a predisposing factor in the development of PAC.

As the main objective of the study was to describe the dark–light changes in iris configuration, we selected only the nasal side for analysis, with the assumption that the dynamic profile is similar in other quadrants. This assumption should be validated in future studies. Because of the scan geometry of the scan probe and the refraction at smooth surfaces of the eye, a built-in dewarping algorithm is included in the Visante OCT to correct for image misalignment. This correction, however, was not available when images were directly analyzed from the video capture. Nevertheless, the true value of iris measurement may not be essential in this study, as analyses were performed in evaluating the association or correlation with other anterior segment parameters measured in the same image.

In summary, there are different dynamic patterns of iris configuration that are related to age, axial length, and the ACA. In addition to ACD, iris bowing is independently associated with angle width. Investigating iris dynamics could provide important information in understanding the risk and mechanism of primary angle closure.

References

1. Foster PJ, Johnson GJ. Glaucoma in China: how big is the problem? *Br J Ophthalmol.* 2001;85:1277–1282.
2. Quigley HA, Broman AT. The number of people with glaucoma worldwide in 2010 and 2020. *Br J Ophthalmol.* 2006;90:262–267.
3. Aung T, Nolan WP, Machin D, et al. Anterior chamber depth and the risk of primary angle closure in 2 East Asian populations. *Arch Ophthalmol.* 2005;123:527–532.
4. Lavanya R, Wong TY, Friedman DS, et al. Determinants of angle closure in older Singaporeans. *Arch Ophthalmol.* 2008;126:686–691.
5. Wojciechowski R, Congdon N, Anninger W, et al. Age, gender, biometry, refractive error, and the anterior chamber angle among Alaskan Eskimos. *Ophthalmology.* 2003;110:365–375.
6. Salmon JF. Predisposing factors for chronic angle-closure glaucoma. *Prog Retin Eye Res.* 1999;18:121–132.
7. He M, Foster PJ, Johnson GJ, et al. Angle-closure glaucoma in East Asian and European people: different diseases? *Eye*. 2006;20:3–12.
8. Lowe RF. Aetiology of the anatomical basis for primary angle-closure glaucoma: biometrical comparisons between normal eyes and eyes with primary angle-closure glaucoma. *Br J Ophthalmol.* 1970;54:161–169.
9. Pavlin CJ, Harasiewicz K, Foster FS. Ultrasound biomicroscopy of anterior segment structures in normal and glaucomatous eyes. *Am J Ophthalmol.* 1992;113:381–389.
10. Ochiai H, Chihara E, Chuman H, et al. Age and increased incidence of "forward bowing" of the iris in normal eyes. *J Glaucoma.* 1998;7:408–412.
11. Nonaka A, Iwawaki T, Kikuchi M, et al. Quantitative evaluation of iris convexity in primary angle closure. *Am J Ophthalmol.* 2007;143:695–697.
12. Shaffer RN, Schwartz A. Gonioscopy. *Surv Ophthalmol.* 1957;2:389–409.
13. Leung CK, Cheung CY, Li H, et al. Dynamic analysis of dark-light changes of the anterior chamber angle with anterior segment OCT. *Invest Ophthalmol Vis Sci.* 2007;48:4116–4122.
14. Leung CK, Li H, Weinreb RN, et al. Anterior chamber angle measurement with anterior segment optical coherence tomography: a comparison between slit lamp OCT and Visante OCT. *Invest Ophthalmol Vis Sci.* 2008;49:3469–3474.
15. Li H, Leung CK, Cheung CY, et al. Repeatability and reproducibility of anterior chamber angle measurement with anterior segment optical coherence tomography. *Br J Ophthalmol.* 2007;91:1490–1492.
16. Radhakrishnan S, Goldsmith J, Huang D, et al. Comparison of optical coherence tomography and ultrasound biomicroscopy for detection of narrow anterior chamber angles. *Arch Ophthalmol.* 2005;123:1053–1059.
17. Quigley HA, Friedman DS, Congdon NG. Possible mechanisms of primary angle-closure and malignant glaucoma. *J Glaucoma.* 2003;12:167–180.

18. Leung CK, Chan WM, Ko CY, et al. Visualization of anterior chamber angle dynamics using optical coherence tomography. *Ophthalmology.* 2005;112:980–984.
19. Gazzard G, Friedman DS, Devereux JG, et al. A prospective ultrasound biomicroscopy evaluation of changes in anterior segment morphology after laser iridotomy in Asian eyes. *Ophthalmology.* 2003;110:630–638.
20. Dorairaj S, Oliveira C, Fose AK, et al. Accommodation-induced changes in iris curvature. *Exp Eye Res.* 2008;86:220–225.
21. Kanadani FN, Dorairaj S, Langlieb AM, et al. Ultrasound biomicroscopy in asymmetric pigment dispersion syndrome and pigmentary glaucoma. *Arch Ophthalmol.* 2006;124:1573–1576.
22. Campbell DG. Pigmentary dispersion and glaucoma: a new theory. *Arch Ophthalmol.* 1979;97:1667–1672.
23. Pavlin CJ, Macken P, Trope GE, et al. Accommodation and iridotomy in the pigment dispersion syndrome. *Ophthalmic Surg Lasers.* 1996;27:113–120.
24. Karickhoff JR. Reverse pupillary block in pigmentary glaucoma: follow up and new developments. *Ophthalmic Surg.* 1993;24:562–563.
25. He M, Lu Y, Liu X, et al. Histologic changes of the iris in the development of angle closure in Chinese eyes. *J Glaucoma.* 2008;17:386–392.